

Planar Defects in β -Alumina

Y. LE CARS

Laboratoire de Chimie Appliquée de l'Etat Solide (E.R.A. 387) 11, rue P. et M. Curie, Paris, 75005, and Centre de Recherches de la Compagnie Générale d'Electricité 91460 Marcoussis, France

D. GRATIAS AND R. PORTIER

Laboratoire de Métallurgie Structurale des Alliages Ordonnés (E.R.A. 221) 11, rue P. et M. Curie, Paris 75005, France

AND

J. THÉRY

Laboratoire de Chimie Appliquée de l'Etat Solide (E.R.A. 387) 11, rue P. et M. Curie Paris 75005, France

Received January 7, 1975

Sodium β -alumina crystals were elaborated by melting of a mixture of Na_2CO_3 and Al_2O_3 or by PbO flux evaporation and were studied by transmission electron microscopy. They exhibit regular planar defects lying in the $\{11.0\}$ prismatic planes. These defects are described as antiphase boundaries for the cationic sublattice with fault vectors $\frac{1}{2}\langle 10.0 \rangle$ (such faults do not affect the anionic sublattice). As a consequence it would be interesting to study precisely the structure of the sodium β cationic lattice in the vicinity of the melting point.

Introduction

β -alumina type sodium aluminates have received a great deal of interest in recent years due to their exceptionally high ionic conductivity (1). Two structures have been found by X-ray diffraction (2, 3):

(i) A nonstoichiometric β -alumina phase exists in the composition range between 5.33 Al_2O_3 - Na_2O and 8.5 Al_2O_3 - Na_2O and is described in the $P6_3/mmc$ space group (hexagonal lattice constants: $a = 5.59 \text{ \AA}$, $c = 22.53 \text{ \AA}$). This structure consists of a packing of spinel type blocks (usually two blocks per unit cell) separated by planes where all

sodium ions are randomly distributed (4-6) (Fig. 1).

(ii) A metastable β'' -alumina structure exists in the same range of composition.

When stabilized by magnesia, its space group, determined on single crystals, is $R\bar{3}m$. Lattice parameters referred to an hexagonal unit cell are: $a'' = 5.59 \text{ \AA}$, $c'' = 33.95 \text{ \AA}$. The unit cell consists of a packing of three spinel blocks similar to those of the β form (7, 8).

In the present paper, only the β -phase has been studied. A study of crystals containing a mixture of β and β'' (epitaxially related) is in progress.

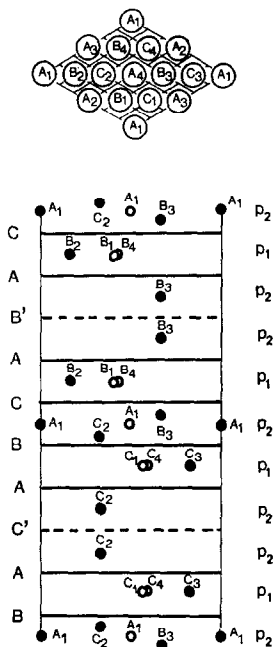


FIG. 1. β -alumina unit cell projected on the (11.0) plane. —, compact layer of oxygen ions; ●, aluminium ions; ----, mirror plane containing one oxygen and the sodium ions.

Experimental

Crystals were elaborated by two methods and identified by X-ray diffraction: (i) by melting a mixture of Na_2CO_3 and Al_2O_3 in appropriate ratio to give the $8.5 \text{ Al}_2\text{O}_3\text{-Na}_2\text{O}$ composition; only β -phase is obtained; and (ii) by PbO evaporation of an analogous mixture (richer in Na_2CO_3) at 1250°C ; β -phase is often found in epitaxy with β'' form. This latter phase has never been obtained alone (9).

Some crystals can be observed directly by transmission electron microscopy. They are thin plates perpendicular to the c direction. In all other cases, samples must be ground before observations, which are performed with a Philips EM 300 100-kV microscope with a goniometer stage.

Results and Discussion

We observed very sharp straight fringes due to planar defects in the three $\{11.0\}$

prismatic planes in every sample. Because of the highly populated reciprocal rows along the c^* direction, standard electron diffraction patterns do not have sufficient accuracy to determine unambiguously the l index values of the spots.

Therefore, a process deduced from radio-crystallographic methods is used: Samples are submitted to an oscillation of about $\pm 15^\circ$ around the goniometer axis of the microscope during the exposure time of the photographic film. Reciprocal rows parallel to the c^* -axis form hyperboloids of revolution which by section with the diffraction plane also generate hyperbolas in the diffraction pattern (Figs. 2a and 2b). The curvature of these hyperbolas, which depends on the chosen rotation axis, is directly measured on the diffraction pattern by the angle of the rotation axis and the hyperbolas' asymptotes. In each projected row, of course, corresponds to the smallest l index, of course, corresponds to the smallest distance from the central spot. These consecutive reciprocal spots parallel to the c^* -axis can always be observed, even if this axis is not in the diffraction pattern.

Hence, two epitaxial structures with one highly populated reciprocal axis—as in β and β'' , for example—can be differentiated, regardless of the orientation of the sample. The l index value of one particular diffraction pattern, taken in the same area and range of rotation as the oscillating pattern, can be determined unambiguously.

As no spots of the β'' -phase are observed in the oscillating diffraction pattern taken in the area where planar defects are present, we conclude that these defects are planar faults in the homogeneous β -phase. A systematic study of the extinction conditions leads to the fault vectors settings given in Table I.

Of course, the same faults are described by the crystallographically equivalent vectors:

$$R_1 = \frac{1}{2}[\bar{1}\bar{2}.0], \quad R_2 = \frac{1}{2}[21.0], \quad R_3 = \frac{1}{2}[\bar{1}\bar{1}.0].$$

They differ from the first ones by a lattice translation and lie in the defect planes.

For the operating Bragg reflections of the reciprocal lattice with h and k even, the three families of defects are always simultaneously

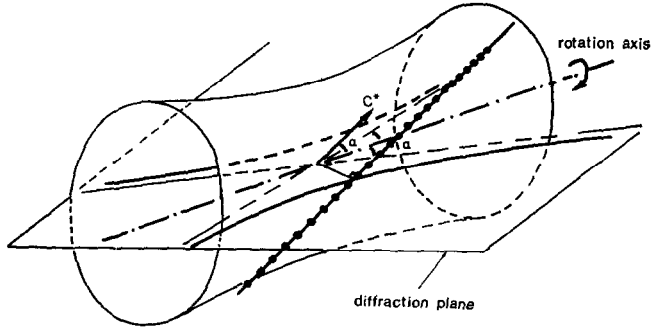


FIG. 2a. Geometrical construction for oscillating crystal electron diffraction pattern.

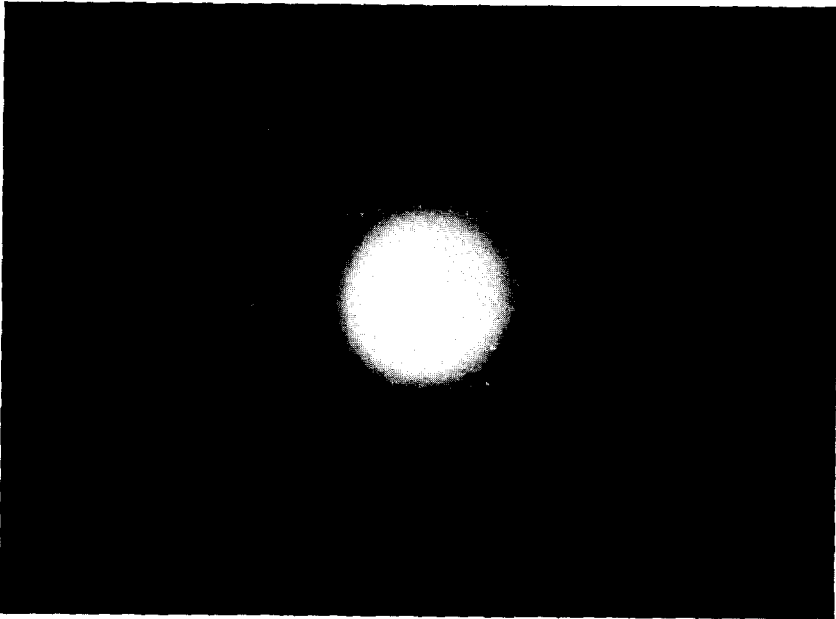


FIG. 2b. Diffraction pattern for the case $\alpha \approx 0$.

out of contrast when observed under two-beam conditions. In all other cases, the phase changes introduced by the defects are $\pm\pi$ for two families; the third is always out of contrast, regardless of the l indice value

TABLE I

	<i>I</i>	<i>II</i>	<i>III</i>
Fault vector	$\frac{1}{2}[10.0]$	$\frac{1}{2}[01.0]$	$\frac{1}{2}[11.0]$
Fault plane	$(2\bar{1}.0)$	$(1\bar{2}.0)$	(11.0)

(Figs. 3a, 3b, and 3c). The π -nature of the defects is clearly exhibited in Figs. 4a and 4b [by comparing the fringe profiles of the bright and dark-field micrographs (10)].

Note that the three fault vectors always transform the *A*, *B*, or *C*-type site into an equivalent site, as shown in Table II. For this reason, if all the positions of one particular type of site are occupied by atoms of the same nature, the fault vectors become fundamental translations for this defined sublattice; this is the case for the oxygen sublattice, which is not modified by the fault (except for the oxygen

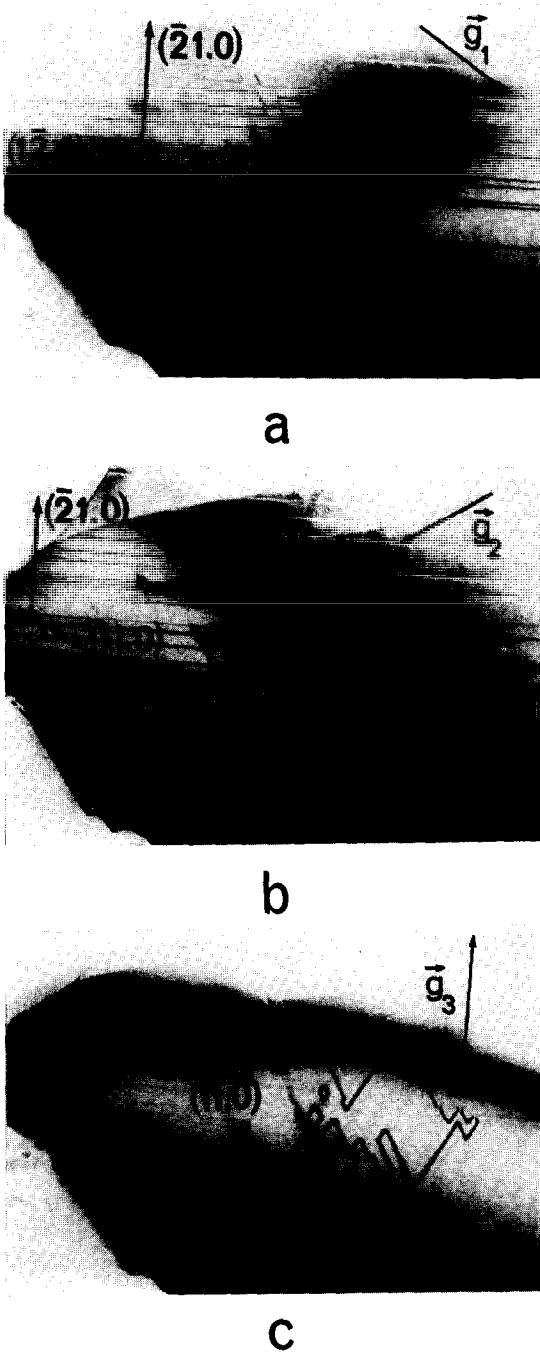


FIG. 3. Typical planar defects in prismatic planes for different operating Bragg reflections. (a) $g_1 = 11.1$. (b) $g_2 = 1\bar{2}.1$. (c) $g_3 = \bar{2}1.1$.

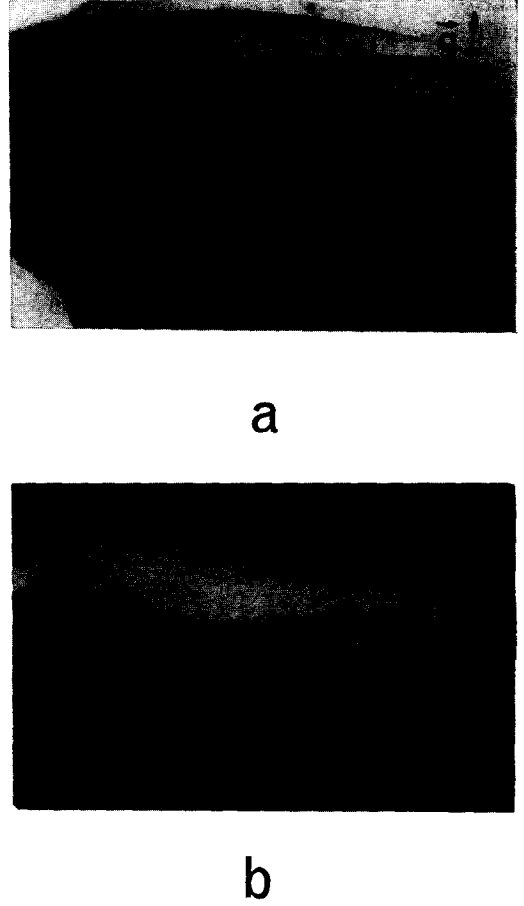


FIG. 4. Symmetrical contrasts of the π fringes between bright and dark fields.

TABLE II
CORRESPONDING SITES BETWEEN THE FOUR ORDERED DOMAINS

$R_1 = \frac{1}{2}\{10.0\}$ $R_2 = \frac{1}{2}\{01.0\}$ $R_3 = \frac{1}{2}\{\bar{1}1.0\}$			
A_1	A_2	A_3	A_4
A_2	A_1	A_4	A_3
A_3	A_4	A_1	A_2
A_4	A_3	A_2	A_1
B_1	B_2	B_3	B_4
B_2	B_1	B_4	B_3
B_3	B_4	B_1	B_2
B_4	B_3	B_2	B_1
C_1	C_2	C_3	C_4
C_2	C_1	C_4	C_3
C_3	C_4	C_1	C_2
C_4	C_3	C_2	C_1

site in the sodium plane). This unmodified sublattice has the symmetry $P6_3/mmc$ with lattice parameters $a/2$, $b/2$, and c . Thus, diffraction spots with h and k even can be considered as fundamental spots, which agrees with the fact that for such operating Bragg reflections every fault is out of contrast.

Hence, only the cationic sublattice will be modified by the fault; two different types of cationic planes are to be considered:

(a) Those for which three sites of the same type are simultaneously occupied (referred to as p_1 in Fig. 1); only two different dispositions of cations are generated by applying the three fault vectors.

(b) Those for which only one site for one determined type is occupied (referred to as p_2 in Fig. 1); here one obtains four different dispositions for the cations.

Thus, four types of equivalent cationic sublattices are possible for the same anionic sublattice; these types can be derived from one another by the three fault vectors. Therefore, the observed planar defects can be described as antiphase boundaries between the four types of ordered domains (referred to as the cationic sublattice).

As a consequence, it would be interesting

to study precisely the structure of the sodium β -alumina in the vicinity of the melting point in order to determine an eventual disordering of the cationic lattice.

References

1. N. WEBER AND J. T. KUMMER, in "Proc. 21st Annual Power Sources Conference, May 1967."
2. G. A. RANKIN AND H. E. MERWIN, *J. Amer. Chem. Soc.* **38**, 568 (1916).
3. J. THÉRY AND D. BRIANÇON, *C.R. Acad. Sci. Paris* **254**, 2782 (1962).
4. W. L. BRAGG, C. GOTTFRIED, AND J. WEST, *Z. Kristallogr.* **77**, 255, 274 (1931).
5. C. A. BEEVERS AND M. A. S. ROSS, *Z. Kristallogr.* **97**, 59 (1937).
6. C. R. PETERS, M. BETTMAN, J. W. MOORE, AND M. D. GLICK, *Acta Crystallogr.* **B27**, 1826 (1971).
7. G. YAMAGUCHI AND K. SUZUKI, *Bull. Chem. Soc. Japan* **41**, 93 (1968).
8. M. BETTMAN AND C. R. PETERS, *J. Phys. Chem.* **73**, 1774 (1969).
9. Y. LE CARS, J. THÉRY, AND R. COLLONGUES, *Rev. Int. Htes Temp. Réfract.* **9**, 153 (1972).
10. S. AMELINCKX, R. GEVERS, G. REMAUT, AND J. VAN LANDUYT, in "Modern Diffraction and Imaging Techniques in Material Science," pp. 257-294, North Holland, Amsterdam, (1969).